

Appendix A to FAR 99-02

**ENERGY INNOVATIONS SMALL GRANT
(EISG) PROGRAM**

EISG FINAL REPORT

VENTILATION MEASUREMENT AND CONTROL

EISG AWARDEE

Federspiel Controls
721 Avila Place
El Cerrito, CA 94530
Phone: (510) 418-3392
Email: cfeders@attglobal.net

AUTHORS

Clifford Federspiel, Principal Investigator

Grant #: 99-02

Grant Funding: \$75,000

Term: September, 1999 – March 15, 2001

PIER Subject Area: Building End Use Energy Efficiency

Legal Notice

This report was prepared as a result of work sponsored by the California Energy Commission (Commission). It does not necessarily represent the views of the Commission, its employees, or the State of California. The Commission, the State of California, its employees, contractors, and subcontractors make no warranty, express or implied, and assume no legal liability for the information in this report; nor does any party represent that the use of this information will not infringe upon privately owned rights. This report has not been approved or disapproved by the Commission nor has the Commission passed upon the accuracy or adequacy of the information in this report.

Inquires related to this final report should be directed to the Awardee (see contact information on cover page) or the EISG Program Administrator at (619) 594-1049 or email eisgp@energy.state.ca.us.

TABLE OF CONTENTS

Abstract.....	1
Executive Summary	2
1 Introduction.....	5
2 Project Approach.....	6
2.1 Mathematical Modeling.....	6
2.2 Sensitivity Analysis	6
2.3 Laboratory-Scale Testing	7
2.3.1 Test Stand.....	7
2.3.2 Design of Prototype	8
2.3.3 Test Conditions	9
2.3.4 Test Procedure.....	10
3 Project Outcomes.....	11
3.1 Mathematical Modeling.....	11
3.2 Sensitivity Analysis	12
3.3 Laboratory-Scale Testing	13
4 Conclusions and Recommendations.....	20
4.1 Conclusions.....	20
4.2 Commercialization Potential.....	21
4.3 Recommendations.....	21
4.4 Benefits to California	21
5 References.....	22
Appendix - Development of Correlation Function	23
Contraction Coefficient and Contraction Velocity	23
Flow Coefficient.....	24
Axial Force	25
Fully-Ducted Systems.....	25
Free-Discharge.....	26
Unducted Intake.....	26
Lateral Force.....	27
Center of Pressure.....	28
Torque	28
Correlation Function.....	29

Abstract

This project involved the development of a torque-based flow measurement (TBFM) technology for ventilation measurement and control. The concept is to use the torque characteristics of control dampers to measure airflow. The hypothesis is that this method should be accurate at low velocity, insensitive to non-uniform flow, inexpensive, and immune to fouling. The technical goal was to achieve an accuracy of $\pm 10\%$ of actual flow or $\pm 5\%$ of full scale, whichever is greater. The project consisted of three basic parts. The first was the development of a correlation function (mathematical model) relating the position, aerodynamic torque, and air velocity. The second was a sensitivity analysis to determine if the technical goal was achievable with typical position and torque measurement errors. The third objective was to design and test a prototype. The mathematical model predicted that the torque characteristic should be solely a function of the damper position. The sensitivity analysis predicted that the technical goal could not be achieved at all positions, but that it could easily be achieved under the most important operating conditions. The tests confirmed that the torque coefficient was independent of the velocity. They also confirmed that the technical goal could not be achieved when the damper was nearly open. The tests showed that the TBFM technology is insensitive to non-uniform flow when the damper is less than 70% open.

Keywords: airflow, control, damper, position, torque, velocity, ventilation

Executive Summary

One of the biggest problems with ventilation controls is that it is difficult to cost-effectively and accurately measure airflow rates, especially at outdoor air intake locations. Typically, outdoor air intakes have no ductwork either upstream or downstream. The most common configuration is a set of dampers mounted in a large opening of a mixing plenum. This configuration can cause large nonuniformities in the velocity distribution, which makes it difficult to use existing airflow technology. Since outdoor airflow rates cannot be measured accurately or cost-effectively, ventilation systems are routinely operated without knowing ventilation rates, and other key airflow variables. The result is that energy is wasted or air quality is compromised, or in some cases both.

The overall technical goal of this project was to develop an energy-efficient, cost-effective, accurate, and maintenance-free flow measurement and control technology for ventilation systems. The specific technical goal is to achieve an accuracy of $\pm 10\%$ of actual flow or $\pm 5\%$ of full scale, whichever is greater. This criterion was derived from an addenda to ASHRAE Standard 62.1. Broader goals include a design that requires less maintenance than current technology and that is inexpensive.

The approach is to use the torque characteristics of control dampers to measure flow. If the position and aerodynamic torque were measured, then it should be possible to deduce the flow rate. The hypothesis is that torque-based flow measurement (TBFM) should be accurate at low velocities if the damper is constructed to induce aerodynamic torque when throttling. The TBFM should also be insensitive to non-uniform flow because the entire surface of the damper blades is used as the sensing means.

This project had three basic objectives. The first was to develop a correlation function (mathematical model) that would accurately relate the position, aerodynamic torque, and air velocity of control dampers. Existing theories on the torque characteristics of butterfly valves were combined with published experimental results to formulate a model that would predict the torque characteristics of multi-blade control dampers.

The second objective was to perform a computer-based sensitivity analysis using the correlation function. The question is whether or not the technical goal could be achieved given typical torque and position measurement errors. The sensitivity of the TBFM technology was compared to the sensitivity of a pitot tube to typical pressure measurement errors.

The third objective was to perform laboratory-scale testing of a prototype to evaluate its performance. A test stand was constructed to test the prototype, and the prototype was designed and constructed based on the results of the modeling and sensitivity analysis. The laboratory tests were designed to assess the accuracy of the TBFM prototype and to assess the impact of non-uniform flow on the performance of the TBFM technology and conventional technology.

The development of the correlation function demonstrated that the relationship between position, torque, and airflow should have a simplified form that makes calibration of the correlation function relatively simple. The correlation function predicts that the velocity is the product of a function of the position and a function of the torque.

The sensitivity analysis showed that the technical goal should not be achievable for all operating conditions, but it should be easily achievable for the most important operating conditions. The sensitivity analysis predicted that the technical goal could not be achieved when the damper was nearly open. The most important operating condition is when the damper is about 10% - 20% open because that is the range of conditions for controlling minimum ventilation. Under that condition, the sensitivity analysis predicted

that the technical goal could be achieved, and that the torque-based flow measurement should significantly outperform a pitot tube or similar flow measurement technology.

The laboratory-scale tests confirmed the results of the sensitivity analysis. A test stand was constructed that used five high-accuracy pitot tubes in a constricted duct as a measurement standard. A prototype with an offset-blade design was constructed. The offset-blade design uses standoffs to make the damper blades rotate about an axis that is displaced by two inches. This design induces torque even when the damper is fully open. The tests showed that when nearly open, the torque was very low even with the offset-blade damper.

Tests were conducted to assess the ability of the TBFM technology to operate accurately in the presence of a flow disturbance. To simulate a disturbance, a commercially available louver was mounted to the frame of the TBFM prototype and to the frame of the commercially available flow station. These tests illustrated that the TBFM technology is insensitive to the flow disturbance when the damper is less than 70% open. When the TBFM damper is more than 70% open, the flow disturbance has a significant negative impact on the accuracy.

The results of Sections 3 and 4 indicate that the TBFM technology can outperform conventional flow measurement technology under a wide range of operating conditions. The results of Section 3 demonstrate that the TBFM technology is more accurate than a pitot tube when the damper is less than 80% open. This result is reinforced by the results of Section 4, particularly the finding that the TBFM technology is insensitive to the presence of a significant upstream flow disturbance when the damper is less than 70% open while the accuracy of a commercially available airflow station was shown strongly affected by the presence of the same upstream disturbance.

The fact that the TBFM technology cannot provide accurate measurement of velocity when the damper is nearly open would be a problem for some applications. For example, if the technology were used to control building pressure by controlling a flow differential between two ducts, then that strategy would fail to operate properly when one or both of the TBFMs was nearly open.

One significant obstacle to commercialization of the TBFM technology is that it cannot be used in the retrofit market. This market is a significant fraction of the HVAC industry. The annual rate of turnover in the commercial building industry is 2%, which means that there are 50 times as many existing air-handling units that could be retrofit as there are new units sold each year. Retrofitting dampers is an expensive proposition. Some are firmly embedded in HVAC units, and could only be replaced by dismantling the HVAC equipment. We contacted a manager from a leading energy service company (ESCO) to get an opinion on the commercial viability of the TBFM. This manager told us that his company would have no interest in the TBFM technology because dampers could not be retrofit cost-effectively.

A significant obstacle to commercialization of the TBFM technology in new construction market is that it requires substantial changes in the way damper technology is designed for it to work properly. At a minimum, low-friction bearings would have to be used. In order to get the full benefit, the damper design would have to be changed to an offset-blade design, which would involve some re-tooling for an equipment manufacturer.

If the technology described in this report were widely used for controlling minimum ventilation in buildings, California would benefit from reduced energy consumption, reduced peak demand, and improved productivity and health. Energy consumption and peak demand would be reduced because the technology would prevent over-ventilation and enable demand-controlled ventilation. Worker productivity and health would be improved because the technology would ensure that acceptable

minimum ventilation was being achieved, which would improve indoor air quality. Fisk and Rosenfeld (1997) estimate that improvements in indoor air quality could save \$12-43 billion nationally in lost productivity due to health problems in buildings.

Follow-on development should focus on reducing the cited obstacle to commercialization in the new construction market and to improving the technical performance when nearly open. One useful study for reducing the obstacle to commercialization in the new construction market might involve studying the extent to which a commercially available control damper could be used for torque-based flow measurement. The technical issue to be solved in that case would be deducing aerodynamic torque in the presence of significant frictional torque because control dampers use bushings rather than low-friction bearings. A useful study for improving the accuracy when wide open might involve investigating a means for periodically increasing the drag coefficient when wide open so that the signal-to-noise ratio would be momentarily improved.

1 INTRODUCTION

One of the biggest problems with ventilation controls is that it is difficult to cost-effectively and accurately measure airflow rates, especially at outdoor air intake locations. Typically, outdoor air intakes have no ductwork either upstream or downstream. The most common configuration is a set of dampers mounted in a large opening of a mixing plenum. This configuration can cause large nonuniformities in the velocity distribution, which makes it difficult to use existing airflow technology. Since outdoor airflow rates cannot be measured accurately or cost-effectively, ventilation systems are routinely operated without knowing ventilation rates, and other key airflow variables. The result is that energy is wasted or air quality is compromised, or in some cases both.

The amount of power required by ventilation systems is correlated with time of day. Cooling power required to condition ventilation air is highest when it is hottest outside. For variable-air-volume systems, flow rates and the associated fan power requirements are highest when cooling loads are highest. These facts imply that inefficient ventilation systems contribute disproportionately to peak electricity demand in the summer. Since problems with insufficient electrical capacity are currently acute in California, there is a significant incentive for focusing efforts on ways to improve the energy efficient operation of ventilation systems. Being able to measure airflow rates is a necessary first step to improving the efficiency.

There are numerous existing methods of measuring airflow. The most common methods include pressure-based devices (pitot tube, orifice plate, venturi meter), heated resistors, tracer gases, rotating vane anemometers, vortex-shedding flow meters, and ultrasonic anemometers. These methods share a number of technical problems that make them poorly suited to ventilation measurement and control. The problems include fouling when the sensing element is in the flow path, sensitivity to non-uniform velocity distribution when the method measures velocity at a point, excessive energy use when the method requires a constriction or obstruction in the flow path, and high cost.

The overall goal of this project is to develop an energy-efficient, cost-effective, accurate, and maintenance-free flow measurement and control technology for ventilation systems. The specific technical goal is to achieve an accuracy of $\pm 10\%$ of actual flow or $\pm 5\%$ of full scale, whichever is greater. This criterion was derived from an addenda to ASHRAE Standard 62.1. Broader goals include a design that requires less maintenance than current technology and that is inexpensive.

The proposed technology is based on fundamental principles of fluid mechanics. As air passes over the blades of control dampers, it exerts an aerodynamic force on the damper blades. This force consists of lift and drag. The lift and drag forces are related to the velocity of the fluid, the geometry of the damper blades, and the configuration of the damper blades. The force can be measured either directly or indirectly. Knowing the magnitude and direction of this force along with the position of the damper blades is sufficient information to determine the flow rate. This technique implies that the control element (i.e., the damper) is also the sensing element.

The proposed method is to measure aerodynamic torque, rather than measure the individual forces. The damper can be constructed with the axle off-center like a backdraft damper so that the aerodynamic force on the blades can be determined from the measurement of the actuation torque. If friction is minimized by using low-friction bearings, then the actuation torque will be approximately equal to the aerodynamic torque. An advantage of measuring torque is that it can be measured inexpensively. For example, it can be determined by measuring the deflection of an elastic coupling between the actuator and damper axle. The position of the damper can be determined either by direct measurement, such as with a potentiometer, or

indirectly such as by counting the steps of a stepper motor. A correlation function can be embedded into a programmable controller that would measure the damper position and actuation torque and then compute the flow rate using the correlation function. Other advantages of using this method to measure and control flow are as follows: (1) it is energy-efficient because it induces no extra pressure loss as an orifice plate would, (2) it should be insensitive to the velocity distribution, so installation costs should be lower, and (3) it cannot be fouled, so maintenance costs should be lower.

The development described in this report is divided into three parts: mathematical modeling, computer-based testing, and laboratory-scale testing. The procedures and results for each of these three parts are described in the next two sections.

2 PROJECT APPROACH

2.1 Mathematical Modeling

The model development involved searching the open literature for patents, articles, and books related to the technology, and using the results from that search to construct a correlation function relating torque, position, and velocity. We found two theoretical papers and several experimental papers that were used for the development of the correlation function. The theoretical articles by Sarpkaya (1959, 1961) and Hassenpflug (1999) and the book by Milne-Thompson (1968), and the experimental articles by Keller and Salzmann (1936), Bleuler (1938), Netsch and Schulz (1950), and Gaden (1951, 1952) were most useful for development of the correlation function. The section of Beckwith et al. (1993) on measurement error analysis?? was used as the basis of the sensitivity analysis.

The mathematical development of the correlation function is described in Section 3.1. The mathematics are based largely on the works of Sarpkaya (1959, 1961) and Hassenpflug (1999). The mathematical model is based on the assumption of irrotational flow. This is a good assumption for control dampers because the sharp leading edge causes the flow to separate at that point.

The mathematical model developed as part of this project allows for multi-blade dampers and dampers with the axles offset from the center of the blade in either a lateral or chord-wise direction. Empirical, explicit functional relationships between the location of the contraction coefficient and the angle of attack of the blades and the center of pressure and the angle of attack of the blades were developed. Explicit functional relationships are necessary for the correlation function to be embedded in a microprocessor.

2.2 Sensitivity Analysis

This section describes the analysis of the sensitivity of the technology to measurement errors. Propagation of uncertainty was used to relate position and torque sensing uncertainties to the TBFM velocity uncertainty, and to relate pressure sensing uncertainty to the velocity uncertainty of a pitot tube. See Beckwith et al., (1993) for a detailed description of propagation of uncertainty.

The relationship between the uncertainty in a variable y that is a function of a number of independent variables u_1, u_2, \dots, u_n is as follows:

$$\Delta y = \left(\left(\frac{\partial y}{\partial u_1} \Delta u_1 \right)^2 + \left(\frac{\partial y}{\partial u_2} \Delta u_2 \right)^2 + \dots + \left(\frac{\partial y}{\partial u_n} \Delta u_n \right)^2 \right)^{\frac{1}{2}} \quad (2-1)$$

where Δy is the uncertainty in y , and Δu_i is the uncertainty in u_i .

We used an uncertainty of 1% of full scale for the position and torque measurements of the TBFM technology and for the pressure measurement of the pitot tube so that a fair comparison could be made between the TBFM technology and pitot tube technology.

2.3 Laboratory-Scale Testing

2.3.1 Test Stand

To perform the laboratory-scale testing, a test-stand was constructed. Figure 2-1 shows a schematic diagram of the test stand. The test section at the inlet is four square feet. The cross-section is reduced to 15 inches by 15 inches so that low velocities can accurately be measured with an array of pitot tubes. The first elbow contains turning vanes. A flow straightener is placed directly after the first elbow to minimize the impact of the bend on the velocity distribution at the pitot tube array. The blower is a centrifugal machine with backward-inclined blades. It is driven by a three-horsepower three-phase motor.

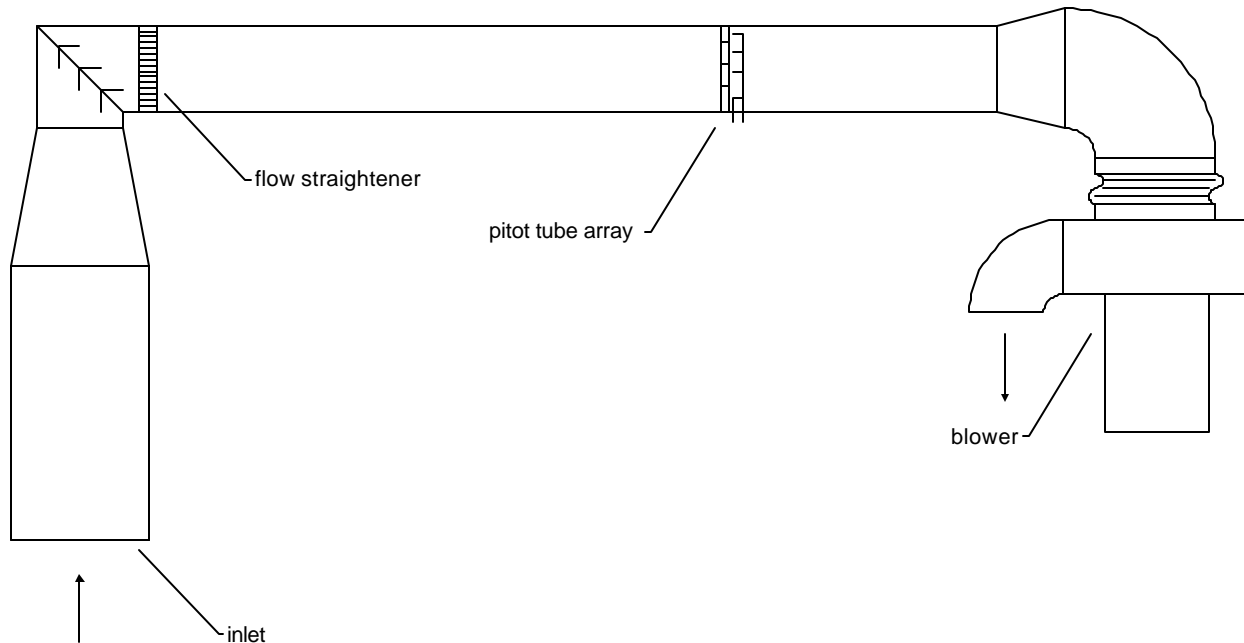


Figure 2-1: Schematic diagram of test stand.

An Altivar 18 variable frequency drive manufactured by Telemecanique/Square D is used to modulate the speed of the blower. A computer with a data acquisition card was used to control the test stand. The data acquisition card is a Data Translation model DT302. Labview version 5.1.1 was used operate the test stand.

The location of the pitot tube array is shown in Figure 2-1. It is two-thirds of the way between the first elbow and the blower. The straight duct in which the pitot tube array is installed is 12.5 feet. The pitot tube array consists of five pitot tubes. One pitot tube was placed at the center of the cross-section of the duct. The other four were placed 1.5 inches from the edges of the duct in each corner. A laboratory quality pressure transducer (Setra model 239) with a span of 1.0 in. w.c. was used to measure the velocity at the center of the duct. This sensor has a rated accuracy of 0.14% of full scale. High-accuracy pressure sensors (Setra model 264) with a rated accuracy of 0.25% of full scale were used to measure the velocities in the corners. The mean velocity was computed by averaging the velocities at the five points.

2.3.2 Design of Prototype

2.3.2.1 Design Criteria

The following criteria were used to determine the design of the prototype

1. Accuracy exceeding that of a pitot tube over the widest possible operating range
2. Acceptable velocity range at all damper positions

The sensitivity analysis demonstrated that it is not possible to achieve the desired accuracy at all positions unless the damper blades have an unreasonably large drag coefficient when wide open. However, the sensitivity analysis also demonstrated that the placement of the axis of rotation relative to the chord of the damper blade has a significant impact on the design criteria.

2.3.2.2 Geometry

The final design of the damper is an “offset-blade” design. The damper blades are offset from the centerline of the axle. The centerline of the damper axles are located at the midpoint of the chord of the damper blades. This resulted in a design that was significantly better than a backdraft damper or a control damper, and that was also easy to construct.

Figure 2-2 shows a photograph of the offset-blade damper mounted on the intake of the test stand. The face area of the damper is four square feet, each side having an internal length of two feet. The damper has four blades. The chord length of each blade is 6-13/16 inches. With this geometry, the angle of attack is 60 degrees when the damper is closed. The damper blades are constructed of polycarbonate plastic that is 0.5 inches thick. The blades have a nominal clearance of 1/16 inch at the sides. The blades are mechanically interlocked with linkages on the outside of the frame. The linkages are designed so that the blades rotate in opposition. The axles rotate in shielded ball bearings pressed into the frame. The linkages also have shielded ball bearings for smooth, low-friction operation.

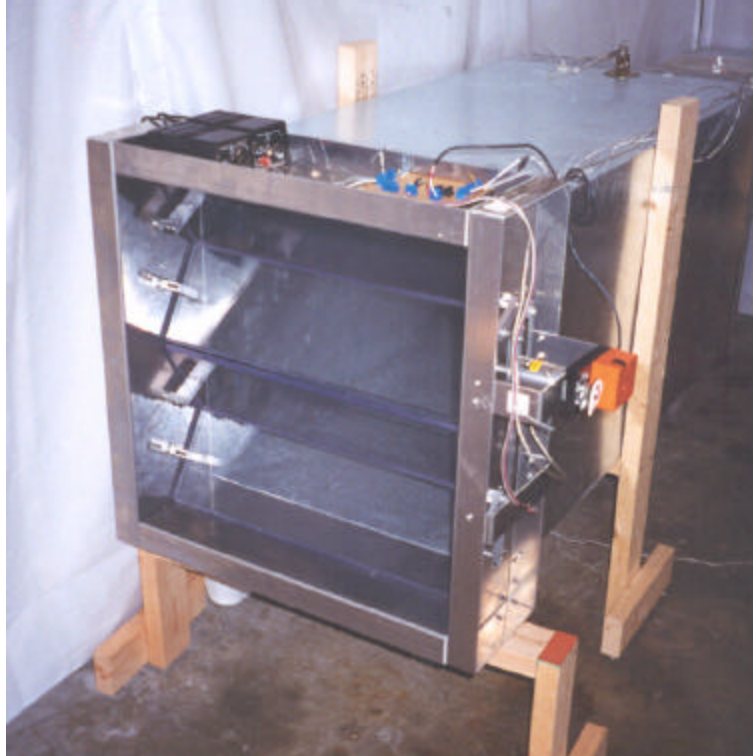


Figure 2-2: Photograph of prototype.

2.3.2.3 Torque and Position Sensors

A commercial, off-the-shelf torque sensor (Futek model T5100) with a span of 100 in-oz was used to measure torque. The sensor has a rated nonlinearity of 0.2% of rated output and a rated hysteresis of 0.2% of rated output. A low-friction potentiometer (Spectrol Model 140) was used to measure the damper position.

2.3.3 Test Conditions

To test the accuracy, five tests were conducted on the prototype and a commercially-available airflow station. The commercially-available flow station was an Air Monitor model Fan-E. This device is a pressure-based flow station. It consists of a manifold for measuring total pressure and a transverse tube for measuring static pressure. The manifold is constructed of round tubes. The dynamic pressure is measured at the front (upstream) of the manifold through a large number of small orifices. The static pressure is measured at a number of points in the transverse tube at an angle of attack of ± 39.5 degrees. This angle is the point at which theoretical fluid flow models predict that the surface pressure on a circular bluff body will equal the static pressure. The flow station has a honeycomb flow straightener mounted in the frame directly upstream of the pressure-sensing manifold and transverse tube. Table 2-1 summarizes the test conditions.

Table 2-1: Test conditions.

	TBFM	Airflow Station
Calibration	1	
Undisturbed Flow	2	3
Disturbed Flow	4	5

Data from Test 1 were used to calibrate the prototype. Data from Test 2 were used to assess the accuracy of the prototype when there was no upstream flow disturbance. Data from Test 3 were used to assess the accuracy of the prototype when operating with an upstream flow disturbance. A commercially-available louver was mounted to the frame of the prototype to induce a flow disturbance. Test 4 was used to assess the accuracy of a commercially-available flow station. Test 5 was used to assess the accuracy of the commercially-available flow station in the presence of the flow disturbance.

2.3.4 Test Procedure

Tests were conducted only after power had been supplied to all instruments for at least one hour. This ensured stable operation of the sensors during each test.

A zero-calibration of all pressure sensors was performed just prior to each test. The appropriate offsets were subtracted with software rather than by adjusting the zero-calibration potentiometers on each sensor. Doing the zero-calibration with software was both faster and more accurate than adjusting the calibration potentiometers.

Prior to each test, the position-sensing potentiometer was calibrated by moving the damper to the fully open and fully closed positions, and then adjusting the calibration curve with software.

Prior to each test a zero calibration of the torque sensor was performed. This involved constructing a nonlinear calibration curve because the mechanical linkages connecting the damper blades induced a gravity torque that was position-dependent. Figure 2-3 shows an example of the torque measurements when the velocity was zero and the zero-calibration curve of the torque sensor for one test.

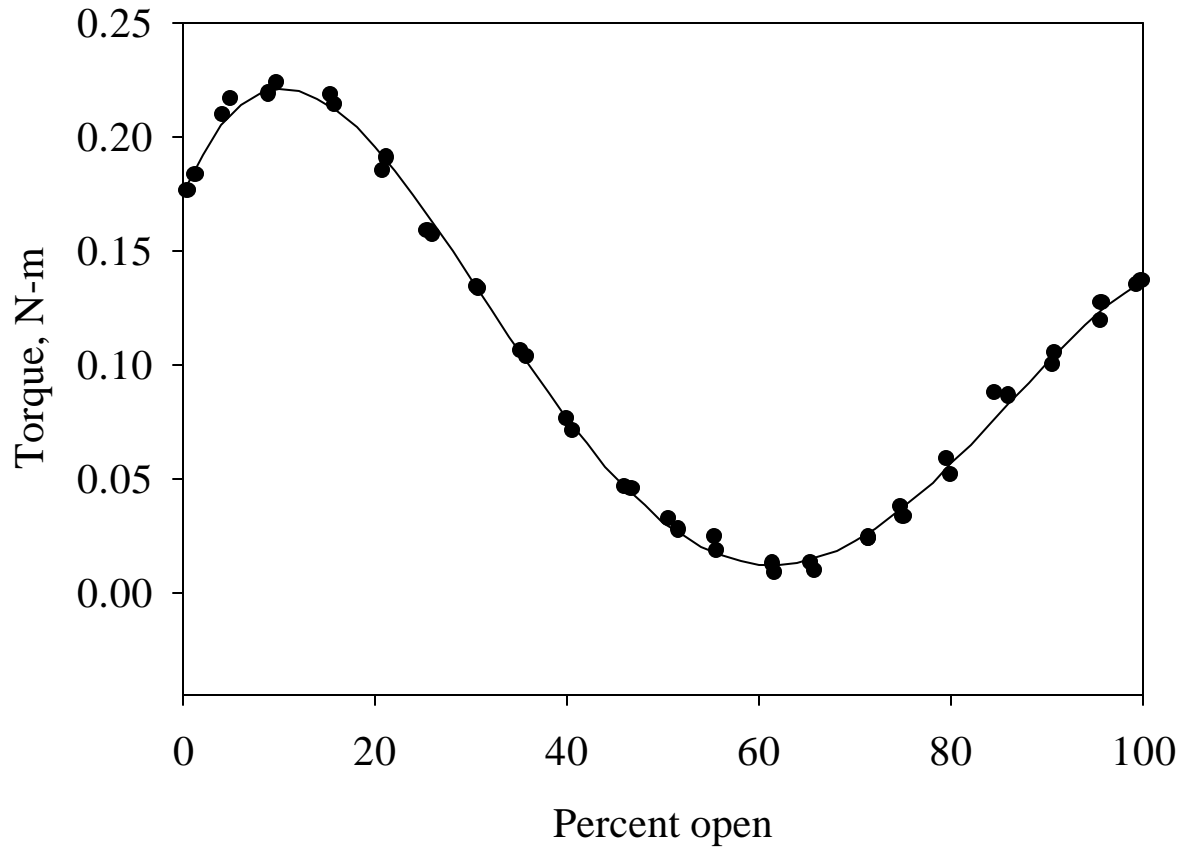


Figure 2-3: Zero-flow calibration curve for torque sensor.

3 PROJECT OUTCOMES

3.1 Mathematical Modeling

The result of the correlation function development is as follows:

$$V = G(\mathbf{a}) \sqrt{\frac{2T}{\mathbf{r}AD}} \quad (3-1)$$

where V is the face velocity, G is the gain, \mathbf{a} is the angle of attack, T is the torque, \mathbf{r} is the density, A is the cross-sectional area, and D is the hydraulic diameter. The model predicts that the gain, which is equal to the inverse of square of the torque coefficient, is solely dependent on the angle of attack. The detailed development of the correlation function can be found in the Appendix.

3.2 Sensitivity Analysis

From equation 3-1, the partial derivative of the velocity with respect to the torque is as follows:

$$\frac{\partial V}{\partial T} = \frac{G(\mathbf{a})}{rADT^{\frac{1}{2}}} \quad (3-2)$$

Similarly, the partial derivative of the velocity with respect to the angle of attack is as follows:

$$\frac{\partial V}{\partial \mathbf{a}} = \frac{\partial G(\mathbf{a})}{\partial \mathbf{a}} \left(\frac{2T}{rAD} \right)^{\frac{1}{2}} \quad (3-3)$$

The partial derivative of the gain with respect to the angle of attack is a complicated function of the angle of attack. To avoid the mathematical complications of computing it analytically, it was computed numerically.

For a pitot tube, the standard error is as follows:

$$E = \frac{\Delta P}{rV} \quad (3-4)$$

where ΔP is the standard pressure measurement error. The velocity at which the standard error equals X% of the maximum flow is as follows:

$$V = \frac{dP}{X} \frac{V_{\max}}{2} \quad (3-5)$$

where dP is equal to ΔP divided by the pressure at the maximum velocity.

Figure 3-1 shows a plot of the velocity at which the accuracy of the proposed technology is the greater of 5% of maximum flow and 10% of reading. In this case the maximum velocity was assumed to be 7.5 m/s. Also shown are the performance of the torque-based velocity measurement applied to a control damper and a backdraft damper with the axle located 20% along the chord from the leading edge of the blade. The offset blade damper outperforms a pitot tube over a wider operating range than a control damper or a backdraft damper, but it does not outperform the pitot tube when nearly open. The control damper is inaccurate both when nearly open and when nearly closed. This is because the center of pressure of the control damper is located exactly at the axle when fully open and when fully closed. This causes the aerodynamic torque of the control damper to be zero for any velocity when fully open or fully closed. The performance of the backdraft damper is worse than the performance of the offset-blade damper because the center of pressure of the backdraft damper is at the axle when fully open.

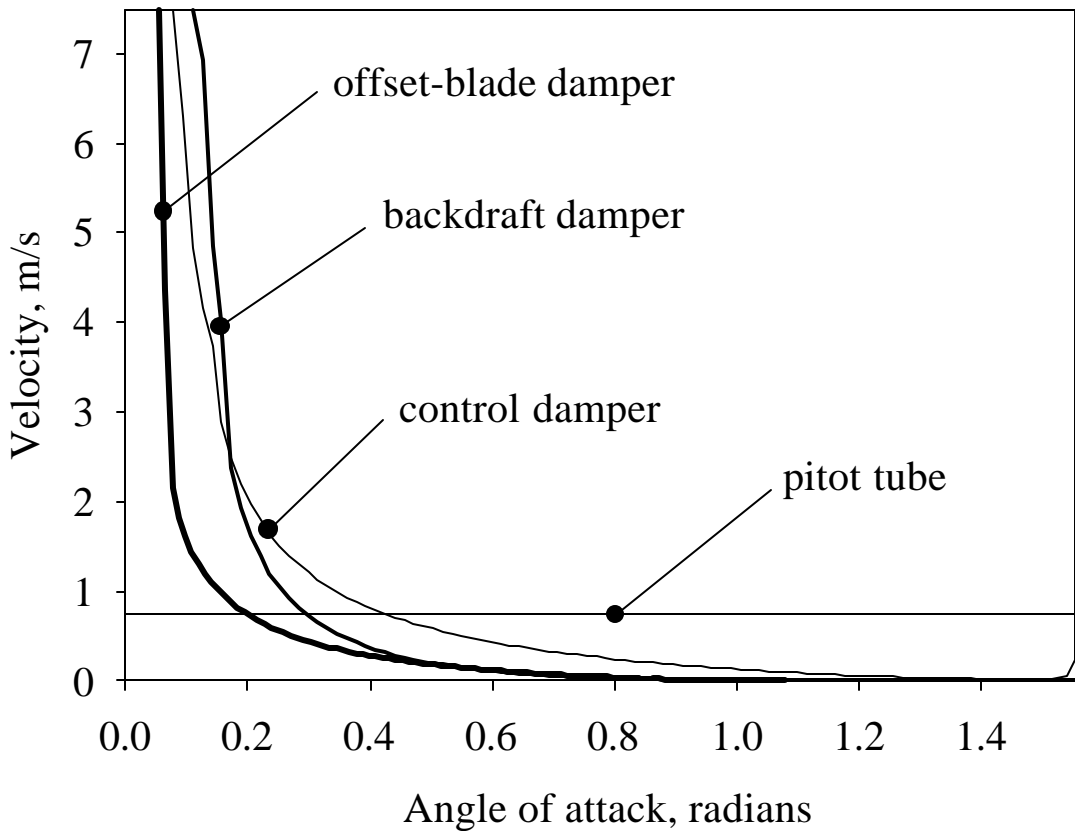


Figure 3-1: Results of sensitivity analysis.

3.3 Laboratory-Scale Testing

Figure 3-2 shows the results of Test 1. The figure shows the computed value of the gain for each of the velocity and position conditions tested. The gain becomes extremely large in the fully-open position. When 100% open, the measured values of the gain were in the range of 12 – 16. The measured values of the torque at 100% open were close to the detection limit of the torque sensor, so the estimates of the gain at 100% open are not accurate. This is consistent with the results of the sensitivity analysis, which predicted high sensitivity to measurement errors when fully open.

The data shown in the figure were used to estimate coefficients of the correlation function. Four coefficients, the drag coefficient of the blades when wide open, the clearance, and gain of the center of pressure function (d_0 in Equation A-24), and exponent of the center of pressure function (n in Equation A-24) were estimated by minimizing the absolute deviation of the correlation function from the measured data using a simplex algorithm. The estimated coefficients are shown in Table 3-1. With these coefficients, Figure 3-2 shows excellent agreement between the measured and predicted gains except when the damper is 100% open.

Table 3-1: Coefficients of the correlation function.

C_D , no units	Clearance, inches	d_0 , no units	n , no units
1.84	0.11	0.25	4.7

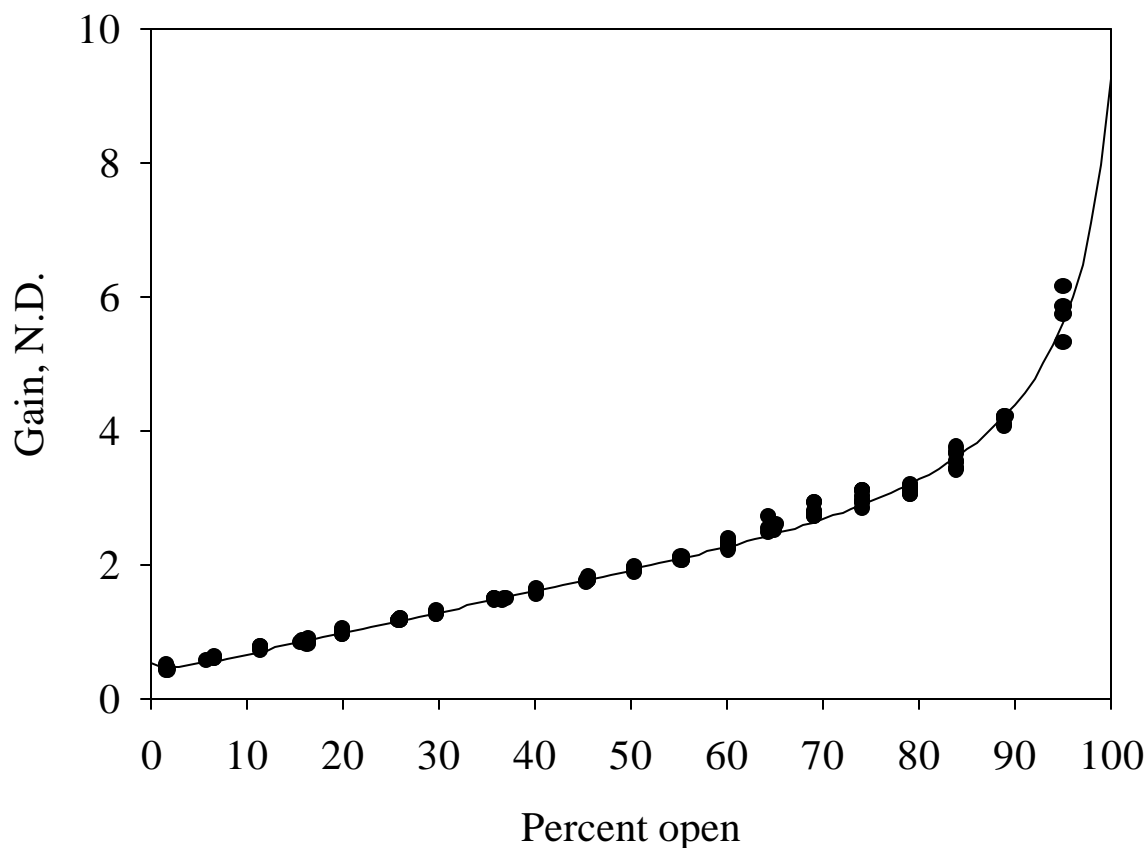


Figure 3-2: Measured and predicted gains versus position.

Figure 3-3 shows the results of Test 2. The calibrated correlation function from Test 1 was used to determine torque-based flow measurements (TBFM) from position and torque readings, and those velocities are compared with the readings from the pitot tube array. The dashed lines in the figure are the bounds of the performance target, which is $\pm 10\%$ of actual flow or $\pm 5\%$ of full scale, whichever is greater. The figure shows that most, but not all, of the points lie within the bounds of the performance target.

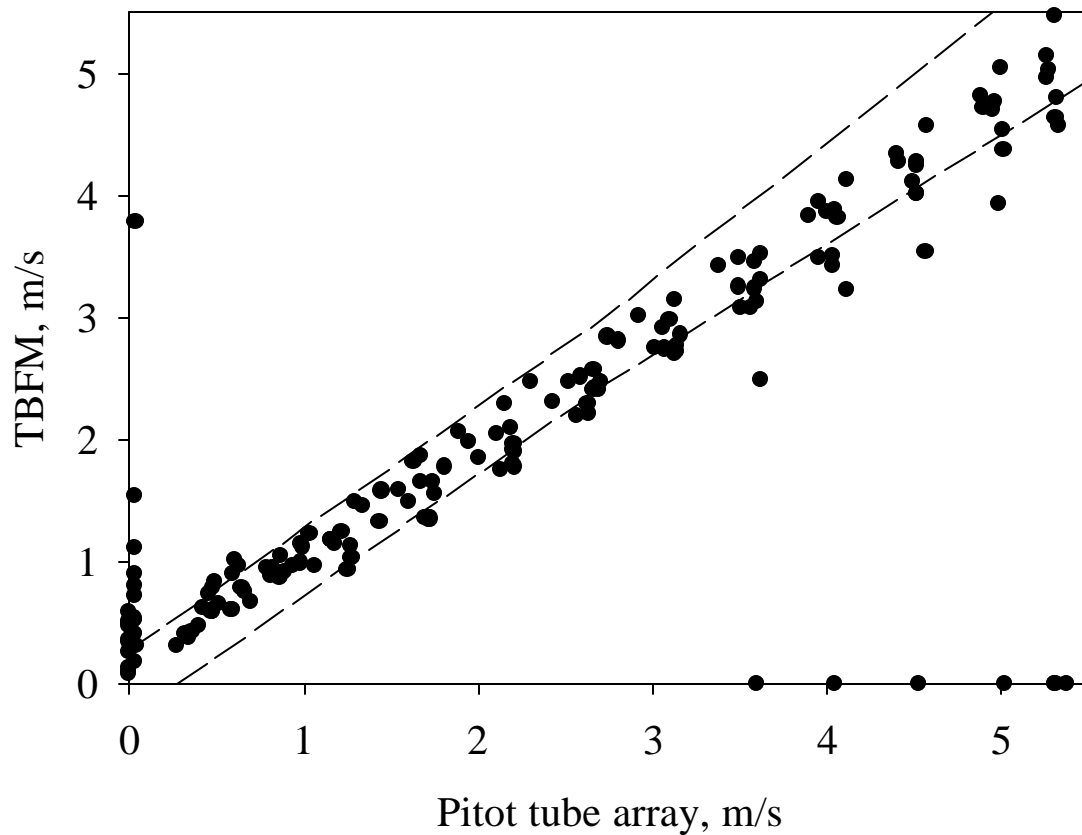


Figure 3-3: TBFM vs pitot tube array

Figure 3-4 shows the difference between the pitot tube readings and the TBFM readings as a function of the position of the damper. The figure illustrates that most of the points that are outside the bounds of the performance target occur when the damper is nearly or completely open. The sensitivity analysis showed that under these conditions the TBFM could not achieve the performance target.

Figure 3-5 shows the results of Test 3. The velocity indicated by the airflow station is compared with the velocity indicated by the pitot tube array. The figure shows that there is a span error that causes more than half of the readings to lie outside of the bounds of the performance target. However, the dispersion of the points is very small, so it would be possible to calibrate the airflow station in such a way that all of the readings lie within the bounds of the performance target.

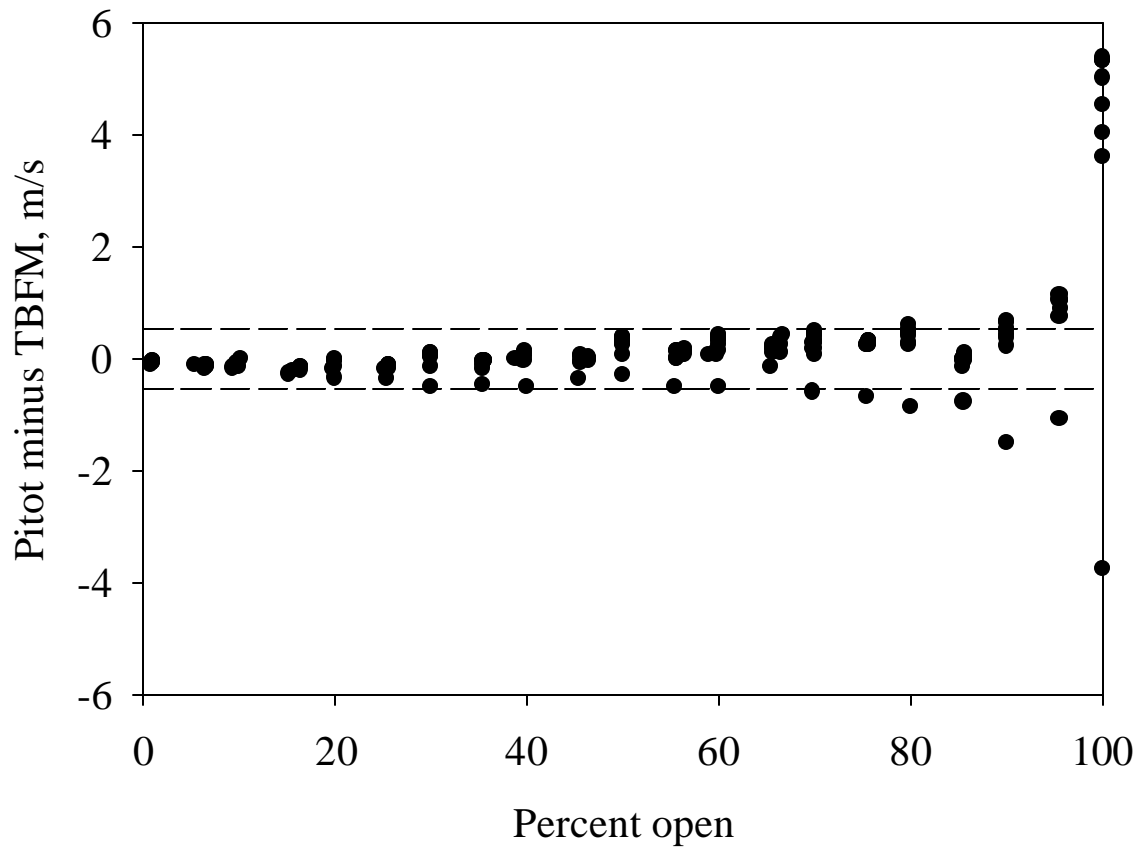


Figure 3-4: Residuals vs position

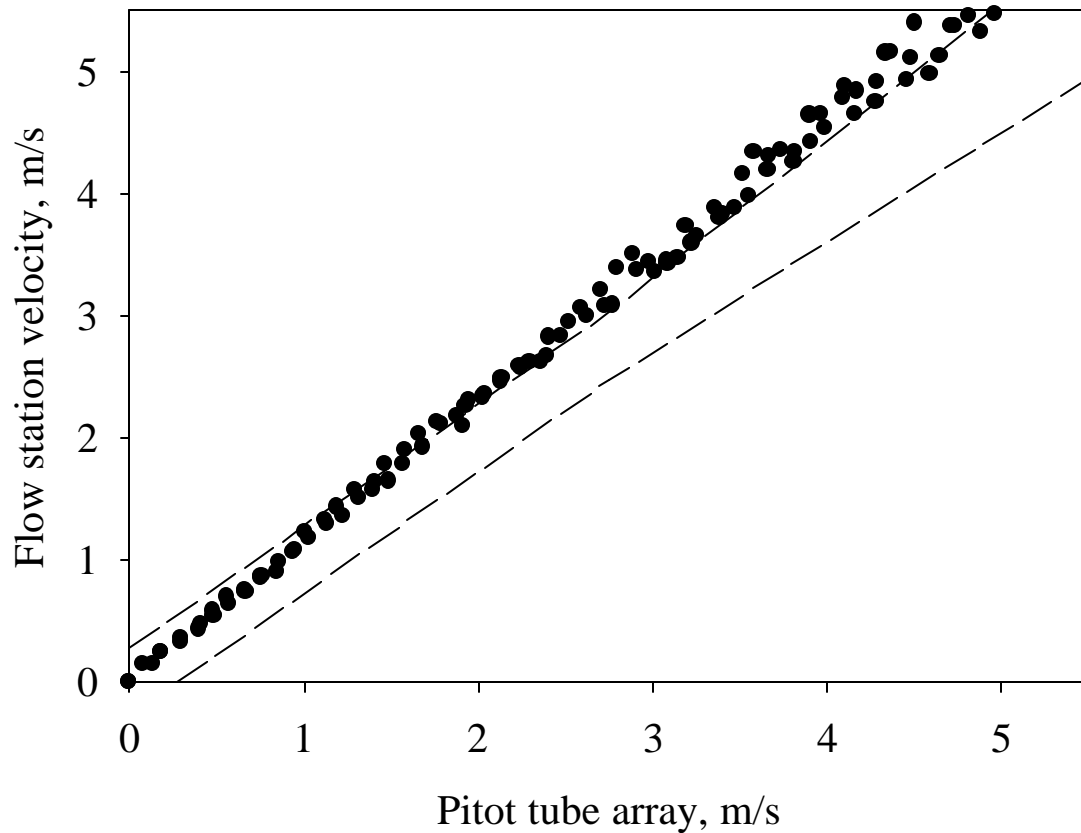


Figure 3-5: Flow station vs pitot tube array; no flow disturbance.

Figure 3-6 shows the results of Test 4. For this test a commercially available louver was mounted directly to the frame of the TBFM upstream of the TBFM device. Like Figure 3-3, most but not all of the points are within the bounds of the performance target. However, the dispersion of the points outside the bounds of the performance target is greater in Figure 3-6 than in Figure 3-3.

Figure 3-7 shows the difference between the pitot tube array and the TBFM as a function of the damper position for Test 4. The figure illustrates that most of the points outside of the performance bounds correspond to conditions when the damper is more than 70% open. When the damper is less than 70% open, the accuracy is generally within the bounds of the performance target.

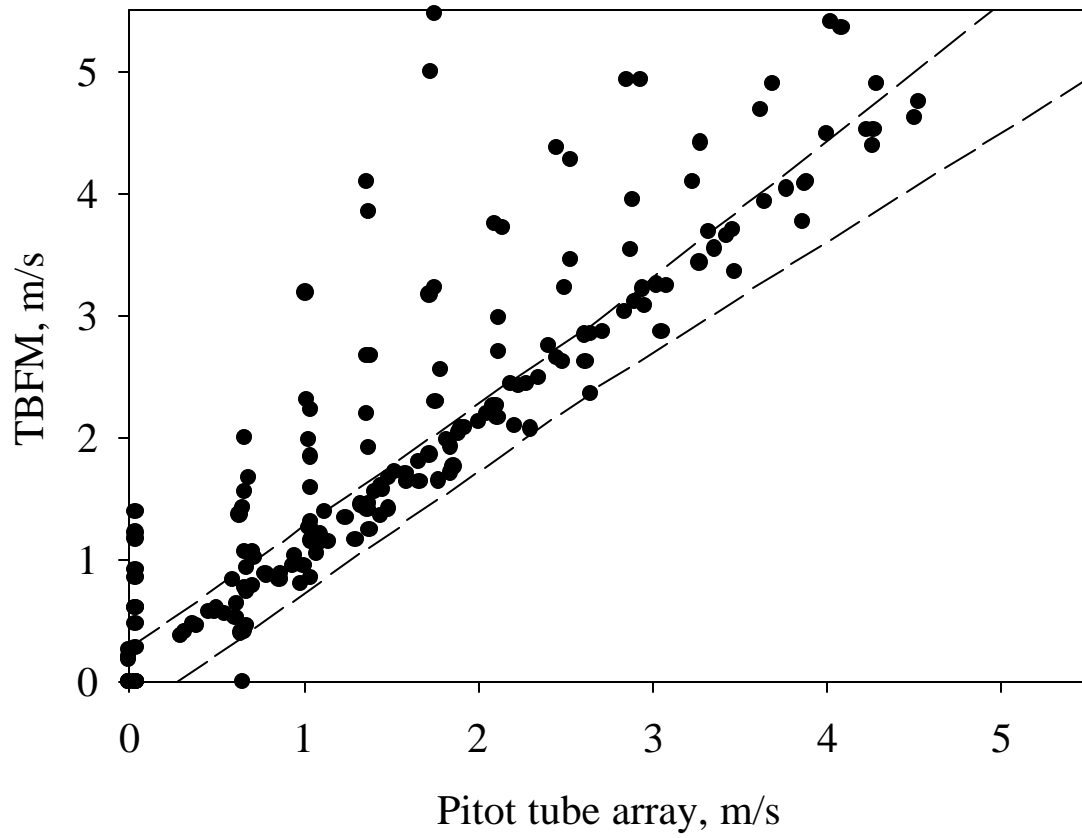


Figure 3-6: Performance of TBFM with upstream flow disturbance.

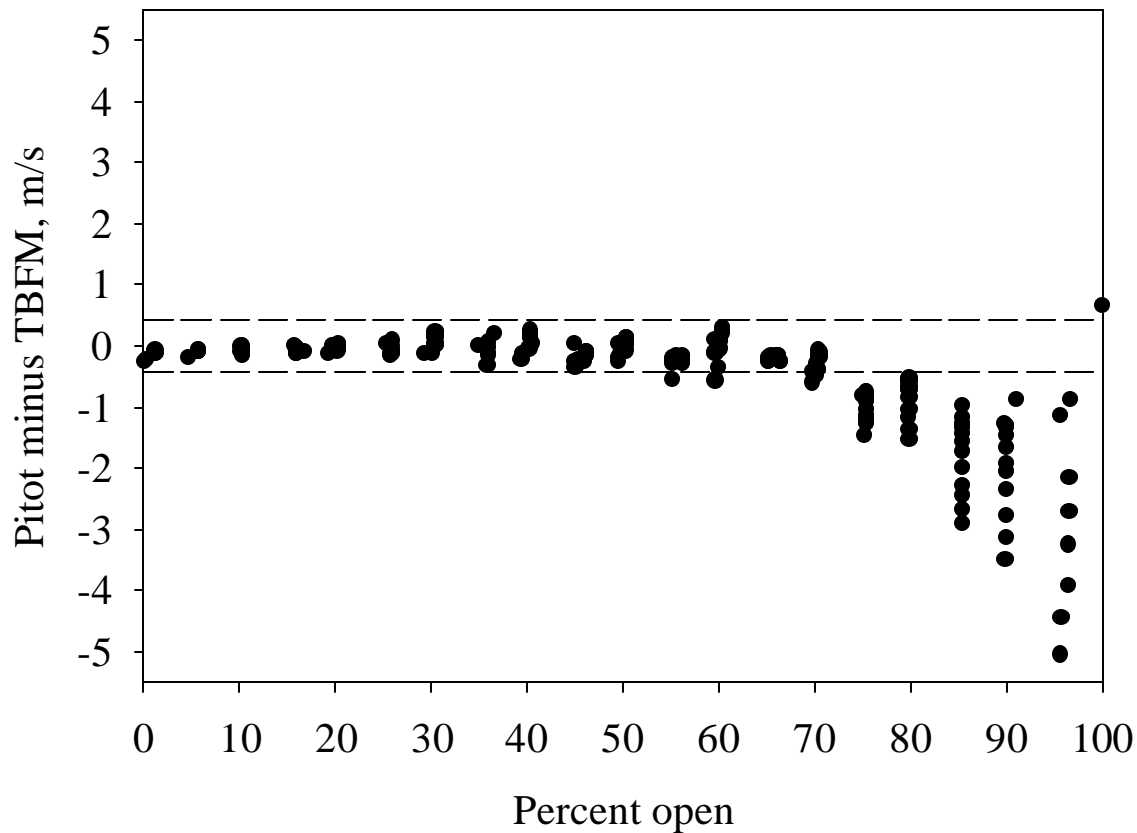


Figure 3-7: Measurement error versus damper position with upstream disturbance.

Figure 3-8, shows the results of Test 5. For this test, a commercially available louver was mounted directly to the frame of the airflow station upstream of the airflow station. Placing a flow disturbance this close to the airflow station violates the installation requirements specified by the manufacturer, and the figure illustrates why. Nearly all of the points are outside the bounds of the performance target. The dispersion of the points is much greater than the dispersion of the points in Figure 3-5, where there was no flow disturbance. Furthermore, if the airflow station had been calibrated to improve its performance in Test 3 it would have made the accuracy even worse in Test 5 because the points were above the bounds of the performance target in Figure 3-5, but are below the bounds of the performance target in Figure 3-8.

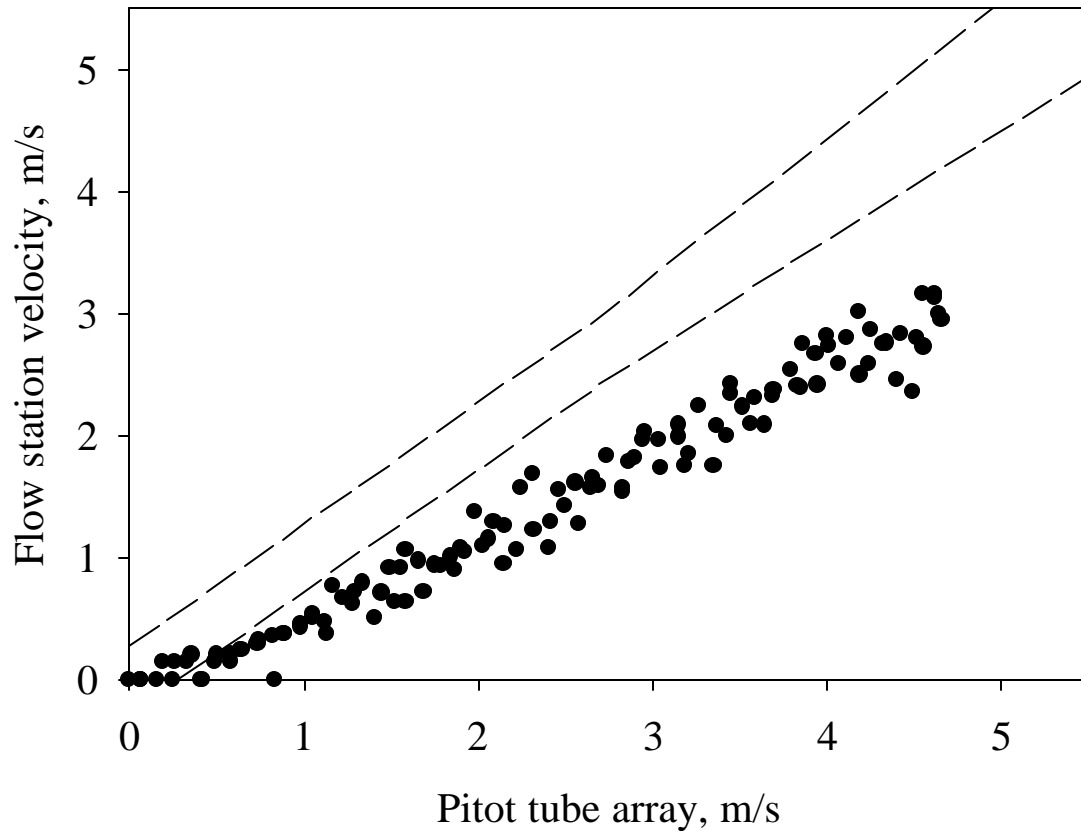


Figure 3-8: Performance of flow station with upstream disturbance.

4 CONCLUSIONS AND RECOMMENDATIONS

4.1 Conclusions

The results of Sections 3 indicate that the TBFM technology can outperform conventional flow measurement technology under a wide range of operating conditions. The results demonstrate that the TBFM technology is more accurate than a pitot tube when the damper is less than 80% open. This result is reinforced by the results of sensitivity analysis, particularly the finding that the TBFM technology is insensitive to the presence of a significant upstream flow disturbance when the damper is less than 70% open while the accuracy of a commercially available airflow station was shown to be significantly negatively impacted by the presence of the same upstream disturbance.

The most important operating condition is when the damper is approximately 10% - 20% open. This is the normal operating condition for an outdoor air damper providing minimum outdoor air. Under this operating condition the TBFM is much more accurate than a pitot tube and is insensitive to flow disturbances.

4.2 Commercialization Potential

The fact that the TBFM technology cannot provide accurate measurement of velocity when the damper is nearly open would be a problem for some applications. For example, if the technology were used to control building pressure by controlling a flow differential between two ducts, then that strategy would fail to operate properly when one or both of the TBFMs was nearly open.

In principle, the TBFM would appear to have cost advantages over conventional technology because torque could be measured with a position sensor and a flexible coupling between the actuator and damper axle. Position sensors are about the least expensive kind of sensor available. However, it is important that the position sensor add little or no friction to the damper mechanism, which increases the cost. Furthermore, the TBFM requires low-friction bearings, which add cost. Consequently, the material costs of the TBFM technology may be comparable to existing technology.

One significant obstacle to commercialization of the TBFM technology is that it cannot be used in the retrofit market. This market is a significant fraction of the HVAC industry. The annual rate of turnover in the commercial building industry is 2%, which means that there are 50 times as many existing air-handling units that could be retrofit as there are new units sold each year. We contacted a manager from a leading energy service company (ESCO) to get an opinion on the commercial viability of the TBFM. This manager told us that his company would have no interest in the TBFM technology because dampers could not be retrofit cost-effectively. Retrofitting dampers is an expensive proposition because some are firmly embedded in HVAC units, and could only be replaced by dismantling the HVAC equipment.

A significant obstacle to commercialization of the TBFM technology in new construction market is that it requires substantial changes in the way damper technology is designed for it to work properly. At a minimum, low-friction bearings would have to be used. Normally control dampers use bushings with much higher friction. In order to get the full benefit, the damper design would have to be changed to an offset-blade design, which would involve some re-tooling for an equipment manufacturer.

4.3 Recommendations

Follow-on development should focus on reducing the cited obstacle to commercialization in the new construction market and to improving the technical performance when nearly open. One useful study for reducing the obstacle to commercialization in the new construction market might involve studying the extent to which a commercially available control damper could be used for torque-based flow measurement. The technical issue to be solved in that case would be deducing aerodynamic torque in the presence of significant frictional torque because control dampers use bushings rather than low-friction bearings. A useful study for improving the accuracy when wide open might involve investigating a means for periodically increasing the drag coefficient when wide open so that the signal-to-noise ratio would be momentarily improved.

4.4 Benefits to California

If the technology described in this report were widely used for controlling minimum ventilation in buildings, California would benefit from reduced energy consumption, reduced peak demand, and improved productivity and health. Energy consumption and peak demand would be reduced because the technology would prevent over-ventilation and enable demand-controlled ventilation. Worker productivity and health would be improved because the technology would ensure that acceptable minimum ventilation was being achieved, which would improve indoor

air quality. Fisk and Rosenfeld (1997) estimate that improvements in indoor air quality could save \$12-43 billion nationally in lost productivity due to health problems in buildings.

5 REFERENCES

- Beckwith, T. G., R. D. Maragoni, and J. H. Lienhard, 1993, *Mechanical Measurements*, Addison-Wesley, New York.
- Bleuler, H., 1938, "Flow Phenomena in Hydraulic Butterfly Valves," *Escher-Wyss News*, 11, 31-35.
- Cohn, S. D., 1951, "Performance Analysis of Butterfly Valves," *Instruments*, 24, 880-884.
- U. S. Department of Energy (DOE), 1999, "Guide for Evaluation of Energy Savings Potential," Office of Building Technology, State and Community Programs.
- Fisk, W.J. and A.H. Rosenfeld. 1997. "Estimates of Improved Productivity and Health from Better Indoor Environments." *Indoor Air*, 7(1), 58-72.
- Gaden, D., 1951, "A Contribution to the Study of Butterfly Valves: Part I," *Water Power*, 3, 456-474.
- Gaden, D., 1952, "A Contribution to the Study of Butterfly Valves: Part II," *Water Power*, 4(1), 16-22.
- Hassenpflug, W. C., 1998, Free-Streamlines, *Computers and Mathematics with Applications*, 36(1), 69-129.
- Keller, C. and F. Salzmann, 1936, "Aerodynamic Model Tests on Butterfly Valves," *Escher-Wyss News*, 9, 3-9.
- Milne-Thomson, L. M., 1968, *Theoretical Hydrodynamics*.
- Ogawa, K. and T. Kimura, 1995, "Hydrodynamic characteristics of a butterfly valve - Prediction of torque characteristics," *ISA Transactions*, 34, 327-333.
- Sarpkaya, T., 1959, "Oblique impact of a bounded stream on a plane lamina," *Journal of the Franklin Institute*, 267, 229-242.
- Sarpkaya, T., 1961, Torque and Cavitation Characteristics of Butterfly Valves, *Journal of Applied Mechanics*, 511-518.

Appendix - Development of Correlation Function

Figure A-1 shows a damper with one blade. The basic principles used here to develop the correlation function are independent of the number of damper blades or their geometrical operation. They can be applied to a multi-blade damper with parallel or opposed blades.

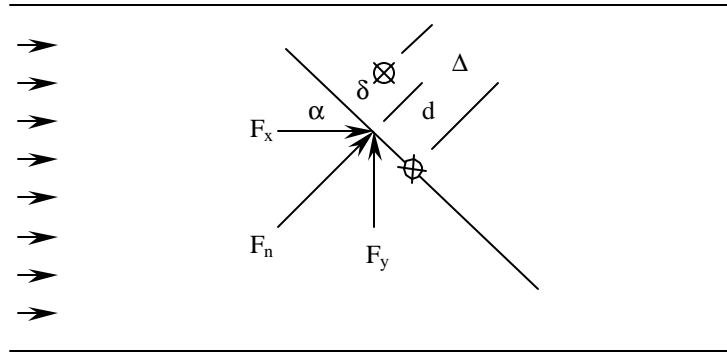


Figure A-1: Schematic diagram of a damper.

Contraction Coefficient and Contraction Velocity

Flow characteristics of dampers are related to the contraction coefficient. The contraction coefficient is defined as the open area at the contraction divided by the apparent open area.

$$C_c = \frac{A_c}{A_a} \quad (\text{A-1})$$

The contraction coefficient is a function of the position of the damper. For simple geometries such as a single-bladed damper, the contraction coefficients can be computed analytically, as has been demonstrated by Sarpkaya (1961) and Hassenpflug (1999). The contraction coefficients can be estimated accurately with polynomial functions. Figure A-2 demonstrates the accuracy that can be achieved with a third-order polynomial. The "data" points are the contraction coefficients computed by Hassenpflug using conformal mapping theory. The maximum difference is just 0.21%.

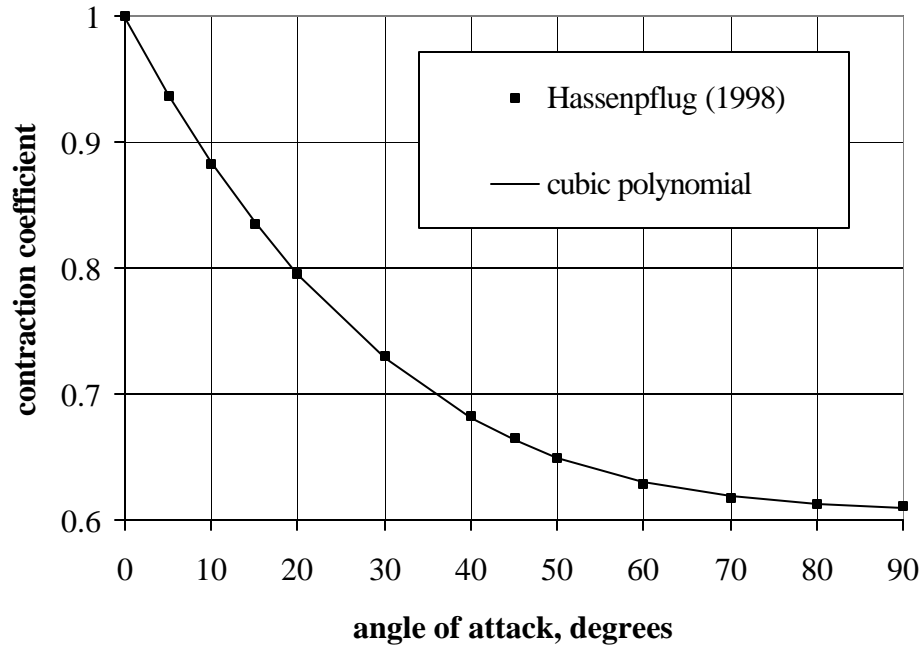


Figure A-2: Contraction coefficient versus angle of attack.

For an incompressible fluid, the velocity at the contraction point is related to the upstream and downstream velocity as follows:

$$\frac{V_u}{V_c} = \frac{A_c}{A_u} = \frac{C_c A_a}{A_u} \quad (\text{A-2})$$

For a rectangular damper with height H , chord length $L/\sin \mathbf{b}$, and blade thickness t , Equation A-2 is as follows:

$$\frac{V_u}{V_c} = \frac{C_c}{H} \left(H - \frac{\sin \mathbf{a}}{\sin \mathbf{b}} L - t \cos \mathbf{a} \right) \quad (\text{A-3})$$

If $L < H$, then the damper leaks when fully closed.

Flow Coefficient

The flow coefficient is defined by the following equation:

$$Q = C_Q A_u \left(\frac{2(P_u - P_d)}{\mathbf{r}} \right)^{\frac{1}{2}} \quad (\text{A-4})$$

The flow coefficient is a function of the position of the damper.

Often, the pressure loss coefficient is used to describe the flow behavior of dampers. The pressure loss coefficient is defined by the following equation:

$$\frac{P_u - P_d}{\mathbf{r}} = K \frac{V^2}{2} \quad (\text{A-5})$$

The loss coefficient can be associated with the upstream velocity, the downstream velocity or the contraction velocity.

When the upstream area equals the downstream area, then the downstream loss coefficient and the flow coefficient are related as follows:

$$K_d = \frac{1}{C_Q^2} \quad (\text{A-6})$$

The pressure loss is assumed to occur due to the sudden expansion after the contraction. The loss coefficient associated with a sudden expansion in a closed conduit has been solved analytically, and can be found in most texts on fluid mechanics. For a closed conduit, the pressure loss is as follows:

$$\frac{P_u - P_d}{\mathbf{r}} = \frac{(V_c - V_d)^2}{2} \quad (\text{A-7})$$

Combining Equations A-2, A-5, and A-7 leads to the following relationship between the flow coefficient, the contraction coefficient, and the open area of the damper

$$C_Q = \frac{C_c A_a}{A_u - C_c A_a} \quad (\text{A-8})$$

Axial Force

Next, three different flow conditions are considered: free-discharge, unducted intake, and fully-ducted.

Fully-Ducted Systems

If the upstream and downstream areas are equal, then the longitudinal force on the damper blade is equal to the pressure difference times the duct area.

$$F_a = (P_u - P_d) A_u \quad (\text{A-9})$$

Combining Equations A-7 and A-9 yields the following:

$$F_a = \frac{\mathbf{r} A_u}{2} (V_c - V_d)^2 \quad (\text{A-10})$$

Substituting Equation A-2 into Equation A-9 and rearranging terms yields the following

$$F_a = \frac{\mathbf{r}A_u V_u^2}{2} \left(\frac{A_u - C_c A_a}{C_c A_a} \right)^2 \quad (\text{A-11})$$

The axial force is related to the flow coefficient in a closed conduit as follows:

$$F_a = \frac{\mathbf{r}A_u V_u^2}{2 C_Q^2} \quad (\text{A-12})$$

Free-Discharge

For free-discharge, the static pressure at the contraction is zero. This implies the following:

$$P_u = \frac{\mathbf{r}}{2} (V_c^2 - V_u^2) \quad (\text{A-13})$$

The momentum equation upstream of the damper is as follows:

$$0 = m(V_u - V_c) + P_u A_u - P_c A_c - F_a \quad (\text{A-14})$$

Substituting Equation A-13 into Equation A-14 and rearranging terms yields the following:

$$F_a = \frac{\mathbf{r}A_u}{2} (V_c - V_u)^2 \quad (\text{A-15})$$

Equation A-15 is equivalent to Equation A-10, so the relationships between the ducted flow coefficient and loss coefficient and the free-discharge axial force are the same as for the fully-ducted axial force.

Unducted Intake

For an unducted intake, the total pressure at the contraction is zero. Also, the static pressure and the velocity well upstream of the damper are both zero. The change in the total head due to the contraction is as follows:

$$H_c - H_d = \frac{(V_c - V_d)^2}{2g} \quad (\text{A-16})$$

The axial force is equal to the change in the total pressure times the downstream duct area.

$$F_a = \frac{\mathbf{r}A_u}{2} (V_c - V_d)^2 \quad (\text{A-17})$$

Equation A-17 is equivalent to Equation A-10. Since Equations A-10, A-15, and A-17 are equivalent, the axial force is independent of the inlet or outlet conditions.

When the angle of attack is zero, the axial force is non-zero due to drag on the open damper blades. The models proposed by Sarpkaya (1961) and Hassenpflug (1999) predict no drag when wide open. Drag is incorporated into the model by assuming a contraction coefficient less than unity when the damper is wide open. The value of the contraction coefficient when the angle of attack is zero is calculated as follows. First define the drag coefficient when open as follows:

$$C_D = \frac{F_a}{\frac{1}{2} \rho V^2 A_f} \quad (\text{A-18})$$

where F_a is the axial force (drag force) when the damper is open, and A_f is the frontal area of the damper blades when open. Combining Equation A-18 with Equation A-11 yields the following quadratic equation relating the contraction coefficient, the drag coefficient, and the geometry (areas) of the damper:

$$C_c^2 (C_D A_f A_a^2 - A_u A_a^2) + C_c (2A_u^2 A_a) - A_u^3 = 0 \quad (\text{A-19})$$

The damper is defined to have a given drag coefficient when wide open, then the corresponding contraction coefficient is computed by solving Equation A-19.

Lateral Force

The lateral force is modeled assuming that the blade is infinitesimally thin so that the contraction coefficient is one when the angle of attack is zero. Under this assumption, the lateral force is related to the angle of attack and the mean velocity as follows:

$$F_l = \frac{\rho V_u^2 A_u}{2C_{Q,l}^2 \tan \alpha} \quad (\text{A-20})$$

The “lateral flow coefficient,” $C_{Q,l}$, is the flow coefficient that for an infinitesimally thin damper blade. The equation for the lateral flow coefficient is as follows:

$$C_{Q,l} = \frac{C_{c,l} A_{a,l}}{A_u - C_{c,l} A_{a,l}} \quad (\text{A-21})$$

The lateral contraction coefficient is unity when the angle of attack is zero. The axial area used to compute the lateral force, $A_{a,l}$, is the area assuming a blade thickness of zero. It is computed as follows:

$$A_{a,l} = H - NW_B \sin \alpha \quad (\text{A-22})$$

When the angle of attack is zero, the lateral force is zero.

Center of Pressure

The distance between the midpoint of the chord of the damper and the center of pressure, which is denoted as d , can be accurately estimated from measured or published data using a trigonometric function. For irrotational flow in an unbounded flow field, Kirchoff proved that the center of pressure is the following function of the angle of attack.

$$\frac{d}{D} = \frac{3}{4} \left(\frac{\cos \mathbf{a}}{4 + \mathbf{p} \sin \mathbf{a}} \right) \quad (\text{A-23})$$

When the angle of attack is zero, the center of pressure is 18.75% from the center of the chord. Sarpkaya (1961) and Ogawa and Kimura (1995) have shown that this is not a good model for flow in a conduit. A generalized version of the relationship between the angle of attack and the location of the center of pressure is as follows:

$$\frac{d}{D} = d_0 \left(\frac{4 \cos \mathbf{a}}{4 + \mathbf{p} \sin \mathbf{a}} \right)^n \quad (\text{A-24})$$

With $d_0 = 0.1875$ and $n = 2$, Figure A-3 shows how Equation A-24 predicts values derived from Sarpkaya (1961). The derived values are the ratio of the measured torque coefficient divided by the theoretical axial force coefficient, where the force coefficient is computed using the contraction coefficients calculated by Hassenpflug (1999).

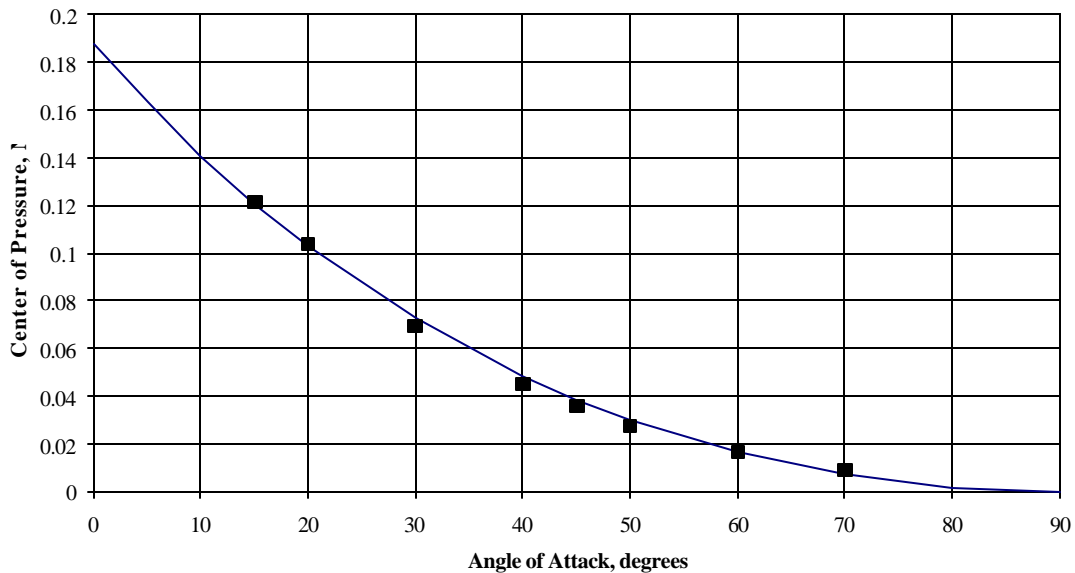


Figure A-3: Center of pressure versus angle of attack.

Torque

The torque required to hold the damper in a fixed position at a give flow rate is as follows:

$$T = F_a y + F_l x \quad (\text{A-25})$$

The lateral and axial distances from the axle to the center of pressure are as follows:

$$y = -\mathbf{d} \cos \mathbf{a} + (\Delta - d) \sin \mathbf{a} \quad (\text{A-26})$$

$$x = (\Delta - d) \cos \mathbf{a} + \mathbf{d} \sin \mathbf{a} \quad (\text{A-27})$$

Correlation Function

A correlation function useful for computing the flow rate based on position and torque measurements can be derived from the equations listed above. When the torque is positive, then the correlation function is as follows:

$$V|V| = G^2(\mathbf{a}) \frac{2T}{rA_u D} \quad (\text{A-28})$$

When the torque is negative, the velocity is negative, and the absolute value of the torque is used in Equation 24 instead of the torque. The gain is a non-dimensional variable that is solely a function of the angle of attack. The equation for the gain is as follows:

$$G(\mathbf{a}) = \left(\frac{D}{\frac{y}{C_{Q,a}^2} + \frac{x}{C_{Q,l}^2 \tan \mathbf{a}}} \right)^{\frac{1}{2}} \quad (\text{A-29})$$

The gain is the inverse of the square of the torque coefficient.